Cytochrome c Oxidase : Remaining Questions About the Catalytic Mechanism

Wikström, Mårten

World Scientific
2019

Wikström , M & Sharma , V 2019 , Cytochrome c Oxidase : Remaining Questions About the Catalytic Mechanism . in J Barber , A V Ruban & P J Nixon (eds) , Oxygen Production and Reduction in Artificial and Natural Systems . World Scientific , Singapore , pp. 135-145 . https://doi.org/10.1142/9789

http://hdl.handle.net/10138/316901
https://doi.org/10.1142/9789813276925_0007

acceptedVersion

Chapter 8

Cytochrome *c* Oxidase — Remaining Questions About the Catalytic Mechanism

Mårten Wikström* and Vivek Sharma*,†

*Institute of Biotechnology, University of Helsinki, Helsinki, Finland
marten.wikstrom@helsinki.fi
†Department of Physics, University of Helsinki, Helsinki, Finland
vivek.sharma@helsinki.fi

Cytochrome *c* oxidase harnesses dioxygen (O_2) as the terminal electron acceptor in the respiratory chains of mitochondria and many aerobic bacteria, and was appropriately named The Respiratory Enzyme (Das Atmungsferment) by Otto Warburg. Its catalytic activity completes the oxygen cycle in biology, which starts by the water-splitting reaction of photosynthesis, amply covered elsewhere in this volume. The mechanism of catalysis of cytochrome *c* oxidase is largely known today, but some uncertainty remains with respect to the ferric/cupric intermediate of the binuclear heme iron/copper centre, which is to be discussed here.

1. Introduction

Spectroscopic data gathered by several laboratories over the last half century has revealed the key aspects of the catalytic mechanism of cytochrome *c* oxidase and identified the corresponding structures of intermediates of the active binuclear centre (BNC), which consists of a heme group, a histidine-ligated copper ion nearby, and a tyrosine residue covalently bonded to one of the copper histidines [Wikström *et al.*, 2018]. The chemical nature of this important tyrosine was first

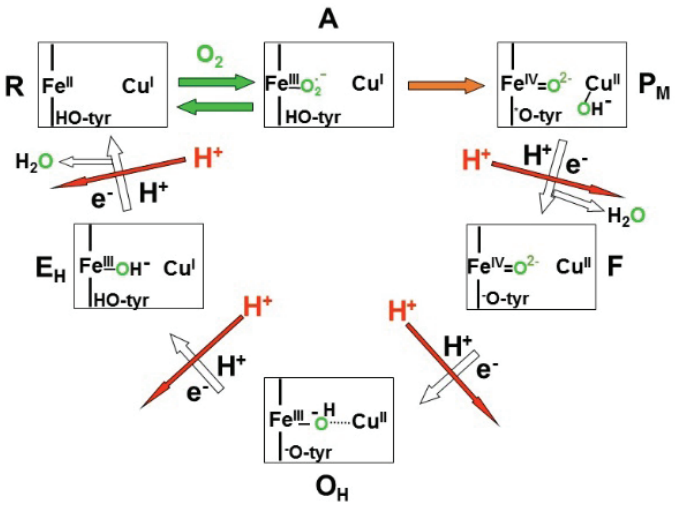

Figure 1. Catalytic cycle of cytochrome *c* oxidase. The rectangular boxes encompass the binuclear centre (BNC), including heme a_3, Cu_B and the tyrosine covalently linked to one of the three histidine ligands of Cu_B (histidines not shown). The name of the catalytic intermediate is given next to the box. Red arrows with protons (H^+) denote proton-pumping events; black H^+ denotes uptake of a "substrate proton". tyr–O* denotes a neutral tyrosine radical. The alternative structure of the activated state $\mathbf{O_H}$ (Fe[III]–-OH^- Cu[I] TyrO*) and relaxation of $\mathbf{O_H}$ to the resting state **O** are not depicted, but later discussed extensively in the text.

reported by Yoshikawa *et al*. on the basis of one of their early X-ray structures of cytochrome *c* oxidase from bovine heart mitochondria [Tsukihara *et al.*, 1996].

Figure 1 depicts the catalytic cycle schematically. The reduced intermediate **R** reacts with O_2 to form the oxygen-bound intermediate **A** (about 10 μs at room temperature and 1 mM O_2) in which charge transfer from heme iron to the ligand makes this a ferric-superoxide structure. In the absence of a donor electron in the adjacent heme *a*, the next step is an exergonic splitting of the O–O bond (*ca*. 200 μs) using two electrons from the heme iron, one from the copper and the fourth from the tyrosine in the active site, which also donates a proton to form the neutral tyrosyl–histidine ligand of Cu[II]. This yields the highly oxidised so-called $\mathbf{P_M}$ state. In contrast, if the donor heme *a* is reduced it delivers the electron to the BNC instead of the tyrosine, which only donates the proton (*ca*. 25 μs). The result is then state $\mathbf{P_R}$ with ferryl heme, Cu[II]–OH^- and tyrosinate anion [Morgan *et al.*, 2001].

It is noteworthy that O_2 binding is highly reversible with a K_D as high as *ca.* 0.3 mM [Chance *et al.*, 1975;Verkhovsky *et al.*, 1994]. By contrast, the conversion of intermediate **A** to $\mathbf{P_M}$ is exergonic with a free energy change of *ca*. –5 kcal/mol [Blomberg, 2016]. The four subsequent reaction steps all involve net uptake of an

electron and a proton to the BNC, and are each linked to pumping of an additional proton from the negatively charged *N*-side of the membrane to the positive *P*-side (red arrows) [Verkhovsky *et al.*, 1999]. In the first of these steps, the **P** intermediate is converted to the **F** state (100–150 μs), and then the latter transforms into state $\mathbf{O_H}$ (*ca*. 1.5–2 ms).

2. The Enigmatic O States

Whilst the BNC structures of intermediates **R**, **A**, $\mathbf{P_M}$, $\mathbf{P_R}$, and **F** are well-established (see above and Figure 1), the structures of the ferric/cupric **O** states ($\mathbf{O_H}$ in Figure 1) still presents problems. Proton translocation (red arrows, Figure 1) has been shown to occur in all four reaction steps associated with transfer of an electron to the BNC [Verkhovsky *et al.*, 1999], but three observations seemed to be in contrast to such a conclusion. First, the injection of an electron into cytochrome *c* oxidase, as isolated, where the BNC is in the resting ferric/cupric state, resulted in fast electron transfer (eT) to heme *a*, but very sluggish further eT to the BNC, and no proton translocation [Verkhovsky *et al.*, 1999; Bloch *et al.*, 2004]. Secondly, classical anaerobic equilibrium redox titrations of cytochrome oxidase, either in mitochondria or of the isolated mitochondrial or bacterial enzyme, showed midpoint redox potentials (E_m) of heme a_3 (Fe[III]/Fe[II]) and Cu_B (Cu[II]/Cu[I]), *i.e*. the two transitions on the left hand side of Figure 1, of less than 400 mV [Gorbikova *et al.*, 2006]. Since the donor, cytochrome *c*, has an E_m of *ca*. 250 mV, the approximate driving force for electron transfer between the donor and the BNC would be only some 150 mV, which is far too low to drive protonic separation of *two* charges across a typical protonmotive force across the membrane of some 200 mV (one of those charges is due to the proton pump; the other from the combination of eT from cytochrome *c* to the BNC and uptake of one proton per electron by the latter to complete oxygen reduction chemistry).

Thirdly, the sum of free energy changes in the catalytic cycle must match the free energy change of the overall reaction, *i.e.* O_2 reduction to water by cytochrome *c*. The approximate E_m values are known from experiments for the two first redox couples, $\mathbf{P_M}$**/F** and **F/O** to be of the order of 800 mV each [Wikström *et al.*, 2018], the free energy change of the conversion of **A** to $\mathbf{P_M}$ is *ca*. –5 kcal/mol (~220 meV) (see above), and the free energy change of O_2 binding (**R**→**A**) is close to zero (see above). This means that the average E_m value of the remaining two redox couples (**O/E** and **E/R**) must be of the order of 690 mV, *i.e*. much higher than measured in redox titrations (<400 mV).

Based on these three findings, we proposed that the ferric/cupric state of the BNC in the resting enzyme (we called it state **O**) is not normally involved in the catalytic cycle, which would instead work with an activated form called $\mathbf{O_H}$.

The subscript H stemmed from the discovery by Rousseau *et al.* [Han *et al.*, 1990] by resonance Raman spectroscopy of a high-spin ferric hydroxy intermediate that followed the **F** state in the catalytic sequence. When electron donation to the enzyme ceases, we proposed that the $\mathbf{O_H}$ state spontaneously relaxes into the **O** state with lower energy and with a considerably lowered E_m. This notion was supported by the finding that electron injection at a sufficiently early stage after oxidation of fully reduced enzyme (~100 ms), indeed led both to fast transfer of the electron to the BNC, to proton pumping, and finally to reduction of Cu_B alone, indicating a much higher E_m than that observed in redox titrations [Bloch *et al.*, 2004; Belevich *et al.*, 2007].

One confusion in the field stems from the fact that the ferric/cupric "as isolated" enzyme (*i.e.* what we here call the **O** form) can in itself exist in different forms, *pulsed vs. resting*, and *slow vs. fast* [Moody *et al.*, 1991]. Here, whilst the structural difference between these forms remains unknown, the fast form has been shown to best correspond to native oxidised enzyme in mitochondria, and the method of its purification is well-established.

In an attempt to test the postulated structural and functional difference between the **O** and $\mathbf{O_H}$ states, Jancura *et al.* [2006] studied the rate of heme a_3 reduction of "fast" bovine cytochrome *c* oxidase by hexaaminеruthenium plus dithionite (reduction of Cu_A and heme *a* is very fast and occurred within the time of mixing in the flow apparatus). The $\mathbf{O_H}$ state was produced by mixing reduced enzyme with O_2 in the presence of the two reductants, whereas reduction of state **O** was assessed by mixing enzyme anaerobically with the reductants. No significant difference in heme a_3 reduction rate was observed in the two conditions. It is noteworthy, however, that the observed rates of heme a_3 reduction were 80–90 s^{-1} in the $\mathbf{O_H}$ conditions, and nearly the same for the state **O** conditions, which is only some 15% of the maximum turnover of bovine enzyme (see *e.g.* [Riegler *et al.*, 2005]). The corresponding rates of heme a_3 and Cu_B reduction deduced from freeze-quench EPR data [Jancura *et al.*, 2006] were only *ca.* 5 s^{-1}. The suspicion thus arises that the employed reductants may have limited the rate and therefore did not reveal the $\mathbf{O_H}$ intermediate.

In a more recent account by Vilhjálmsdóttir *et al.* [2018] the complex of cytochrome *c* with cytochrome *c* oxidase was tested for the occurrence of state $\mathbf{O_H}$. In this system the fully reduced oxidase was supplemented with an additional electron in the form of the bound cytochrome *c*. It was thus expected that when the enzyme reacted with O_2 it would immediately have an additional electron available after forming the activated $\mathbf{O_H}$ intermediate, and thus lead to a situation in which Cu_B has a high redox potential and would readily accept that electron. However, the optical spectroscopic experiments revealed no preference for reduction of Cu_B. In contrast, the "extra electron" was mainly distributed between

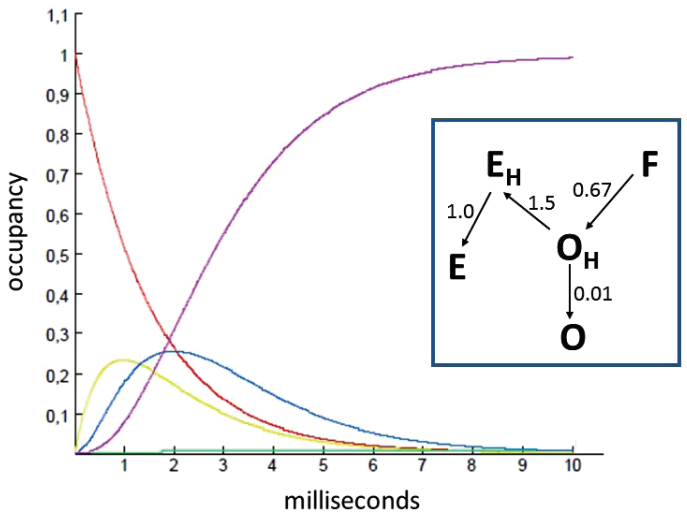

Figure 2. Hypothetical fate of the $\mathbf{O_H}$ intermediate in the experiment by Vilhjálmsdóttir *et al.* [2018]. The insert in the marked square shows a possible reaction scheme of what may happen after primary relaxation of the **F** state into $\mathbf{O_H}$. The numbers denote approximate reaction velocities in ms^{-1}. All reactions are assumed to be irreversible for simplicity. The graph shows a simulation of this system with the **F** state (red trace) fully occupied initially. The other curves show the time dependence of the **E** state (purple), the $\mathbf{E_H}$ state (blue), the $\mathbf{O_H}$ state (yellow), and the **O** state (green).

cytochrome *c*, Cu_A and heme *a*, with preference for the latter, but with very little contribution from the BNC, which remained highly oxidised.

This experimental approach is interesting, and we can only suggest one reason for why it may not have revealed the nature of the $\mathbf{O_H}$ state.

Figure 2 (inset) shows a scheme of how the **F** intermediate (see Fig. 1) turns into $\mathbf{O_H}$, and then how $\mathbf{O_H}$ might initially be converted to an activated (and hypothetical) $\mathbf{E_H}$ state, which relaxes into an **E** state, where redox potentials correspond to those found in anaerobic equilibrium redox titrations. As shown in Figure 2 (main panel), under the kinetic conditions of the scheme (insert) the $\mathbf{E_H}$ state with a high redox potential for Cu_B would not be sufficiently occupied to be observed in the experiments by Vilhjálmsdóttir *et al.* [2018].

3. The Structures of the $\mathbf{O_H}$ and O States

Earlier, based on density functional theory (DFT) calculations [Sharma *et al.*, 2013], we suggested a structure of the activated $\mathbf{O_H}$ state of the BNC (see Figure 1) in which the Cu_B center possesses a high redox potential necessary to catalyze redox-coupled proton pumping in the $\mathbf{O_H} \rightarrow \mathbf{E_H}$ transition of the catalytic cycle (see [Verkhovsky *et al.*, 1999; Bloch, *et al.*, 2004]). In a considerable fraction of

this structure, Cu_B attains a cuprous (Cu[I]) electronic character together with an unpaired electron on the cross-linked Tyr, formally written as Fe[III]–OH^- Cu[I] TyrO*. In this state it was observed that the distance between Cu and Fe is reduced to *ca.* 4Å, and that the hydroxy ligand of Fe is also a weak ligand of Cu, forming a μ-hydroxo bridge between the metals, also observed in a number of compounds synthesized to mimic the oxidase active site [Obias *et al.*, 1998; Hematian *et al.*, 2015]. Later on, Blomberg and Siegbahn [2015], reached the same structure of the active site in the $\mathbf{O_H}$ state, and remarkably similar results were also obtained by computational studies of the structurally similar active site of the ba_3 oxidase from *Thermus thermophilus* [Du and Noodleman, 2015]. In contrast to the overall good agreement on the structure of the active site in the $\mathbf{O_H}$ state, the identity of the relaxed **O** state remains less certain. In our earlier work, we suggested that the structure of the **O** state is (Fe[III]–OH_2 $^-$HO–Cu[II] $TyrO^-$) with a proton being shared between the OH groups of the two metals. A similar structure of the **O** state was initially proposed by Blomberg and Siegbahn based on DFT calculations [Blomberg and Siegbahn, 2014]. However, in their later studies [Blomberg and Siegbahn, 2015] it was suggested that state **O** may have the two-hydroxy structure Fe[III]–OH^- $^-$HO–Cu[II] TyrOH, which despite being higher in energy than state $\mathbf{O_H}$, has lower redox potential of the active site, a characteristic in agreement with experimental data. Two additional structures of **O** states were further considered, $\mathbf{O_B}$ and $\mathbf{O_P}^+$, the latter with an extra proton in the BNC [Blomberg and Siegbahn, 2015]. Because no magnetic coupling was found for the two-hydroxy structure, and its higher energy, it was concluded that the $\mathbf{O_P}^+$ structure (Fe[III]–OH^-…Cu[II] TyrOH) is the best candidate for the relaxed **O** state with a calculated exchange coupling (J) of ~114 cm^{-1} [Blomberg and Siegbahn, 2015].

By using the available coordinates of the two-hydroxy **O** and $\mathbf{O_H}$ states [Blomberg and Siegbahn, 2015], we performed single-point DFT calculations using the B3LYP functional [Becke, 1993; Lee *et al.*, 1988] and the def2-TZVP basis sets [Weigend and Ahlrichs, 2005] (dielectric constant of 4 with dispersion corrections [Grimme *et al.*, 2010]), and constructed a state similar to our earlier proposal of the **O** state structure, *viz.* (Fe[III]–OH_2 $^-$HO–Cu[II] $TyrO^-$). We again (*cf.* [Sharma *et al.*, 2013]) found the latter shared-proton-structure to be *ca.* 16 kcal/mol lower in energy than the two-hydroxy **O** state, which is at the same energy level as the $\mathbf{O_H}$ state (high spin) in agreement with our earlier estimates [Sharma *et al.*, 2013], as well as with those of Blomberg and Siegbahn [2015]. Moreover, we further tested our models [Sharma *et al.*, 2013] by removing an extra water molecule that hydrogen bonded the oxygenous ligands of the metals to tyrosine, and then found the $\mathbf{O_H}$ state to be *ca.* 10 kcal/mol higher in energy than the **O** state (Fe[III]–OH_2 $^-$HO–Cu[II] $TyrO^-$), which has no unpaired electron on

tyrosine in contrast to the $\mathbf{O_H}$ state. Overall, the data supports the idea that (Fe[III]–OH_2 $^-$HO–Cu[II] $TyrO^-$) could be the relaxed **O** state with a low redox potential of Cu_B due to no unpaired spin on tyrosine and due to the copper hydroxyl ligand. When we calculate the magnetic coupling constant (J) of this state using the Yamaguchi formulation [Soda *et al.*, 2000], we find it to be *ca.* 7 cm^{-1}. This weak exchange coupling is actually in excellent agreement with the most recent experimental observations [Oganesyan *et al.*, 1998; Hunter *et al.*, 2000; Cheesman *et al.*, 2004], which suggest, in contrast to previous belief, that the magnetic coupling in the fully oxidised relaxed state of the heme-copper oxidases is very weak, of the order of ~1 cm^{-1}. Interestingly, this is also in line with the extent of magnetic coupling of *ca.* 4–6 cm^{-1} between iron and copper in the $\mathbf{P_R}$ intermediate [Morgan *et al.*, 2001].

4. Peroxide in the Active Site?

X-ray structures of cytochrome *c* oxidase from different sources have been interpreted to have a peroxide ligand bridging ferric Fe and cupric Cu in the BNC (see [Andersson *et al.*, 2017] for citations) in the state that we have named state **O** here. Yoshikawa *et al.* [1998], who first made this suggestion, have made it very clear that the resting ferric/cupric state in which a peroxide is postulated is not a state of the enzyme active in catalysis. Indeed, there is no proposal available about how a ferric/cupric peroxide state **O** would fit any reasonable catalytic mechanism. Yoshikawa *et al.* [Mochizuki *et al.*, 1999] reported that titration of the bovine enzyme revealed uptake of six and not four reducing equivalents on full reduction of enzyme in state **O**, in support of a peroxide ligand. Earlier work by others (references in [Mochizuki *et al.*, 1999]) had reported uptake of four reducing equivalents, but Yoshikawa *et al.* ascribed those findings to contamination of the earlier non-crystalline enzyme preparations with iron. However, that would hardly explain the classical data of Vanneste [1966], which was based on pyridine hemochrome determination. In addition, Mitchell *et al.* [1992] found that by reducing bovine heart oxidase with carbon monoxide, or treating enzyme in state **O** with hydrogen peroxide, two or three protons were taken up on forming the **P** and **F** states, respectively, from state **O** (see Figure 1), which is incompatible with an initial ferric/cupric peroxide structure. Bränden and co-workers [Andersson *et al.*, 2017] recently reported the structure of cytochrome ba_3 from *Thermus thermophilus*, using serial femtosecond crystallography with lipid cubic phase microcrystals at room temperature. This work, which showed a single water or hydroxide between the metals in the BNC, also provides an ample summary of the X-ray data of the binuclear site of heme-copper oxidases collected from different species and by different techniques.

5. Discussion

The $\mathbf{O_P}^+$ structure (Fe[III]–OH^-…Cu[II] TyrOH) suggested by Blomberg and Siegbahn [Blomberg and Siegbahn, 2015] as the best alternative for the relaxed **O** state is *ca*. 6.5 kcal/mol lower in energy compared to the $\mathbf{O_H}$ state. However, the extra proton in the BNC is a source of problems. First, FTIR experiments [Gorbikova *et al.*, 2008] have shown that the pK_a of the tyrosine is ~6.6 in the **O** state, indicating that only a small fraction of the tyrosine may be protonated at the neutral or slightly alkaline pH of most experiments. Secondly, the extra proton would increase the net charge of the BNC to +2. Actually, we should include the heme a_3 propionates in such an assessment, in which case the total charge of the BNC is zero in all intermediates of the catalytic cycle known so far. In the $\mathbf{O_H}$ state, for example, the ferric (+3), porphyrinate (−2) and hydroxide (−1) yields a charge of zero, and the cupric copper (+2) plus tyrosinate (−1), gives a total charge of +1. However, whilst the charge of the heme a_3 D-propionate is neutralised by a conserved arginine residue, the negative charge of the A-propionate is not, so that the overall charge is zero. To invoke an additional charge in the BNC (as in the $\mathbf{O_P}^+$ structure) would be expected to be very costly in such a low dielectric environment (see *e.g.* [Kaila *et al.*, 2010]). Thirdly, the source of the postulated extra proton is problematic. Just a little less than two protons are known to be taken up from the external medium on oxidation of the fully reduced enzyme [Mitchell *et al.*, 1992; Mitchell and Rich, 1994], and uptake of one proton each must be attributed to the **P**→**F** and **F**→$\mathbf{O_H}$ steps (Figure 1) (the slight downward deviation from two protons can be attributed to the weak proton–electron linkages of the redox transitions of the two hemes and of Cu_A).

The relaxed **O** state structure that we are suggesting (Fe[III] –OH_2 $^-$HO–Cu[II] $TyrO^-$) is at least 10 kcal/mol lower in energy than the $\mathbf{O_H}$ state, exhibits the deprotonated tyrosinate in accordance with FTIR data (see above), and has a redox midpoint potential considerably lower than the $\mathbf{O_H}$ state. It is presumably formed from the "activated" $\mathbf{O_H}$ state after diffusion of a water molecule from the apolar cavity next to the BNC into the active site [Sharma *et al.*, 2013].

Acknowledgements

VS acknowledges computing time support from the Center for Scientific Computing, Finland, and financial support from the Academy of Finland, the Sigrid Jusélius Foundation and the University of Helsinki. MW is indebted to the Magnus Ehrnrooth Foundation and Societas Scientiarum Fennica for financial support, and to the Nanyang Technolgical University for their hospitality.

References

Andersson, R., Safari, C., Dods, R., Nango, E., Tanaka, R., Yamashita, A., Nakane, T., Tono, K., Joti, Y., Båth, P., Dunevall, E., Bosman, R., Nureki, O., Iwata, S., Neutze, R. and Brändén, G. (2017). Serial femtosecond crystallography structure of cytochrome *c* oxidase at room temperature, *Sci. Rep.*, 7, 4518.

Becke, A.D. (1993). Densityfunctional thermochemistry. III. The role of exact exchange, *J. Chem. Phys.*, 98, 5648–5652.

Belevich, I., Bloch, D.A., Belevich, N., Wikström, M. and Verkhovsky, M.I. (2007). Exploring the proton pump mechanism of cytochrome *c* oxidase in real time, *Proc. Natl. Acad. Sci. USA*, 104, 2685–2690.

Bloch, D., Belevich, I., Jasaitis, A., Ribacka, C., Puustinen, A., Verkhovsky, M.I. and Wikström, M. (2004). The catalytic cycle of cytochrome *c* oxidase is not the sum of its two halves, *Proc. Natl. Acad. Sci. USA*, 101, 529–533.

Blomberg, M.R. (2016). Mechanism of oxygen reduction in cytochrome *c* oxidase and the role of the active site tyrosine, *Biochemistry*, 55, 489–500.

Blomberg, M.R. and Siegbahn, P.E. (2014). Proton pumping in cytochrome *c* oxidase: Energetic requirements and the role of two proton channels, *BBA-Bioenergetics*, 1837, 1165–1177.

Blomberg, M.R. and Siegbahn, P.E. (2015). How cytochrome *c* oxidase can pump four protons per oxygen molecule at high electrochemical gradient, *BBA-Bioenergetics*, 1847, 364–376.

Blomberg, M.R. and Siegbahn, P.E. (2015). Protonation of the binuclear active site in cytochrome *c* oxidase decreases the reduction potential of CuB, *BBA-Bioenergetics*, 1847, 1173–1180.

Chance, B., Saronio, C. and Leigh, J. (1975). Functional intermediates in the reaction of membrane-bound cytochrome oxidase with oxygen, *J. Biol. Chem.*, 250, 9226–9237.

Cheesman, M.R., Oganesyan, V.S., Watmough, N.J., Butler, C.S. and Thomson, A.J. (2004). The nature of the exchange coupling between high-spin Fe(III) heme *o3* and CuB(II) in *Escherichia coli* quinol oxidase, cytochrome *bo3*: MCD and EPR studies, *J. Am. Chem. Soc.*, 126, 4157–4166.

Du, W.-G.H. and Noodleman, L. (2015). Broken symmetry DFT calculations/analysis for oxidized and reduced dinuclear center in cytochrome *c* oxidase: Relating structures, protonation states, energies, and Mössbauer properties in ba3*Thermus thermophilus*, *Inorg.Chem.*, 54, 7272.

Gorbikova, E.A., Vuorilehto, K., Wikström, M. and Verkhovsky, M.I. (2006). Redox titration of all electron carriers of cytochrome *c* oxidase by Fourier transform infrared spectroscopy, *Biochemistry*, 45, 5641–5649.

Gorbikova, E.A., Wikström, M. and Verkhovsky, M.I. (2008). The protonation state of the cross-linked tyrosine during the catalytic cycle of cytochrome *c* oxidase, *J. Biol. Chem.i*, 283, 34907–34912.

Grimme, S., Antony, J., Ehrlich, S. and Krieg, H. (2010). A consistent and accurate ab initio parametrization of density functional dispersion correction (DFT-D) for the 94 elements H-Pu, *J. Chem. Phys.*, 132, 154104.

Han, S., Ching, Y.-C. and Rousseau, D.L. (1990). Ferryl and hydroxy intermediates in the reaction of oxygen with reduced cytochrome *c* oxidase, *Nature*, 348, 89–90.

Hematian, S., Garcia-Bosch, I. and Karlin, K.D. (2015). Synthetic heme/copper assemblies: toward an understanding of cytochrome *c* oxidase interactions with dioxygen and nitrogen oxides, *Acc. Chem. Res.*, 48, 2462.

Hunter, D.J.B., Oganesyan, V.S., Salerno, J.C., Butler, C.S., Ingledew, W.J. and Thomson, A.J. (2000). Angular dependences of perpendicular and parallel mode electron paramagnetic resonance of oxidized beef heart cytochrome *c* oxidase, *Biophys. J.*, 78, 439–450.

Jancura, D., Berka, V., Antalik, M., Bagelova, J., Gennis, R.B., Palmer, G. and Fabian, M. (2006). Spectral and kinetic equivalence of oxidized cytochrome *c* oxidase as isolated and "activated" by reoxidation, *J. Biol. Chem.*, 281, 30319–30325.

Kaila, V.R., Verkhovsky, M.I. and Wikström, M. (2010). Proton-coupled electron transfer in cytochrome oxidase, *Chem. Rev.*, 110, 7062–7081.

Lee, C., Yang, W. and Parr, R.G. (1988). Development of the Colle-Salvetti correlation-energy formula into a functional of the electron density, *Phys.Rev. B*, 37, 785.

Mitchell, R. and Rich, P.R. (1994). Proton uptake by cytochrome *c* oxidase on reduction and on ligand binding, *BBA-Bioenergetics*, 1186, 19–26.

Mitchell, R., Mitchell, P. and Rich, P.R. (1992). Protonation states of the catalytic intermediates of cytochrome *c* oxidase, *BBA-Bioenergetics*, 1101, 188–191.

Mochizuki, M., Aoyama, H., Shinzawa-Itoh, K., Usui, T., Tsukihara, T. and Yoshikawa, S. (1999). Quantitative reevaluation of the redox active sites of crystalline bovine heart cytochrome *c* oxidase, *J. Biol. Chem.*, 274, 33403–33411.

Moody, A.J., Cooper, C.E. and Rich, P.R. (1991). Characterisation of 'fast'and 'slow'forms of bovine heart cytochrome-*c* oxidase, *BBA-Bioenergetics*, 1059, 189–207.

Morgan, J.E., Verkhovsky, M.I., Palmer, G. and Wikström, M. (2001). Role of the PR intermediate in the reaction of cytochrome *c* oxidase with O_2, *Biochemistry*, 40, 6882–6892.

Obias, H.V., van Strijdonck, G.P., Lee, D.-H., Ralle, M., Blackburn, N.J. and Karlin, K.D. (1998). Heterobinucleating ligand-induced structural and chemical variations in [(L)FeIII−O−CuII]$^+$ μ-oxo complexes, *J. Am. Chem. Soc.*, 120, 9696–9697.

Oganesyan, V.S., Butler, C.S., Watmough, N.J., Greenwood, C., Thomson, A.J. and Cheesman, M.R. (1998). Nature of the coupling between the high-spin Fe(III) heme and CuB(II) in the active site of terminal oxidases: Dual-mode EPR spectra of fluoride cytochrome *bo3*, *J. Am. Chem. Soc.*, 120, 4232–4233.

Riegler, D., Shroyer, L., Pokalsky, C., Zaslavsky, D., Gennis, R. and Prochaska, L.J. (2005). Characterization of steady-state activities of cytochrome *c* oxidase at alkaline pH: mimicking the effect of K-channel mutations in the bovine enzyme, *BBA-Bioenergetics*, 1706, 126–133.

Sharma, V., Karlin, K.D. and Wikström, M. (2013). Computational study of the activated OH state in the catalytic mechanism of cytochrome *c* oxidase, *Proc. Natl. Acad. Sci. USA*, 110, 16844–16849.

Soda, T., Kitagawa, Y., Onishi, T., Takano, Y., Shigeta, Y., Nagao, H., Yoshioka, Y. and Yamaguchi, K. (2000). *Ab initio* computations of effective exchange integrals for H–H, H–He–H and Mn_2O_2 complex: comparison of broken-symmetry approaches, *Chem. Phys. Lett.*, 319, 223–230.

Tsukihara, T., Aoyama, H., Yamashita, E., Tomizaki, T., Yamaguchi, H., Shinzawa-Itoh, K., Nakashima, R., Yaono, R. and Yoshikawa, S. (1996). The whole structure of the 13-subunit oxidized cytochrome *c* oxidase at 2.8 Å, *Science*, 272, 1136.

Vanneste, W.H. (1966). The stoichiometry and absorption spectra of components *a* and a_3 in cytochrome *c* oxidase, *Biochemistry*, 5, 838–848.

Verkhovsky, M.I., Jasaitis, A., Verkhovskaya, M.L., Morgan, J.E. and Wikström, M. (1999). Proton translocation by cytochrome *c* oxidase, *Nature*, 400, 480–483.

Verkhovsky, M.I., Morgan, J.E. and Wikstroem, M. (1994). Oxygen binding and activation: Early steps in the reaction of oxygen with cytochrome *c* oxidase, *Biochemistry*, 33, 3079–3086.

Vilhjálmsdóttir, J., Gennis, R.B. and Brzezinski, P. (2018). The electron distribution in the "activated" state of cytochrome *c* oxidase, *Sci. Rep.*, 8, 7502.

Weigend, F. and Ahlrichs, R. (2005). Balanced basis sets of split valence, triple zeta valence and quadruple zeta valence quality for H to Rn: Design and assessment of accuracy, *Phys. Chem. Chem. Phys.*, 7, 3297–3305.

Wikström, M., Krab, K. and Sharma, V. (2018). Oxygen activation and energy conservation by cytochrome *c* oxidase, *Chem. Rev.,* 118, 2469–2490.

Yoshikawa, S., Shinzawa-Itoh, K., Nakashima, R., Yaono, R., Yamashita, E., Inoue, N., Yao, M., Fei, M.J., Libeu, C. P. and Mizushima, T. (1998). Redox-coupled crystal structural changes in bovine heart cytochrome *c* oxidase, *Science*, 280, 1723–1729.